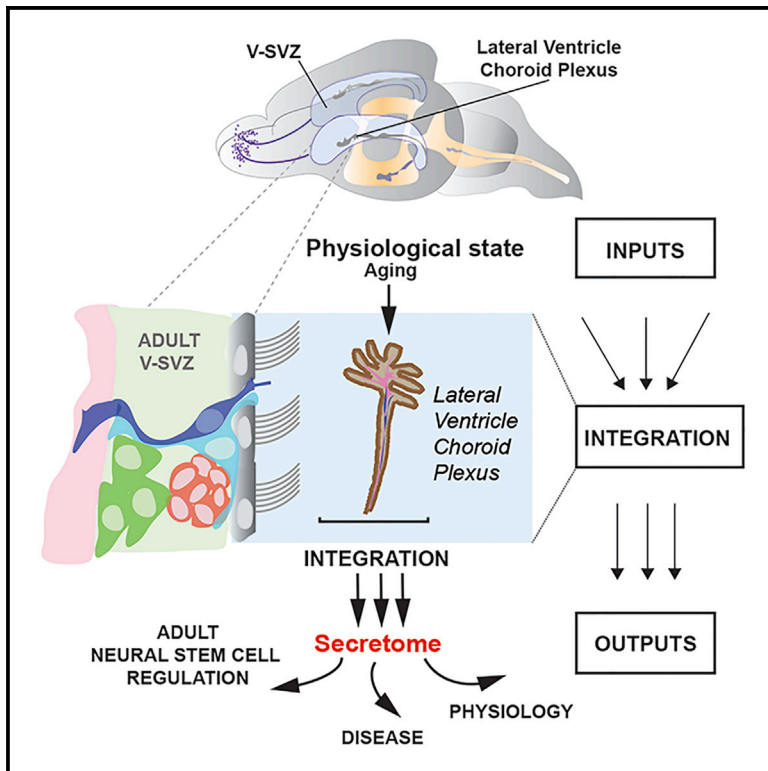


# Cell Stem Cell

## Age-Dependent Niche Signals from the Choroid Plexus Regulate Adult Neural Stem Cells

### Graphical Abstract



### Authors

Violeta Silva-Vargas,  
Angel R. Maldonado-Soto,  
Dogukan Mizrak, Paolo Codega,  
Fiona Doetsch

### Correspondence

fiona.doetsch@unibas.ch

### In Brief

Silva-Vargas et al. show that the lateral ventricle choroid plexus is a novel niche component for adult V-SVZ neural stem cells and their progeny and exhibits dynamic changes with aging.

### Highlights

- The lateral ventricle choroid plexus is a novel component of the adult V-SVZ niche
- LVCP secretome supports the recruitment and proliferation of NSCs and their progeny
- NSCs are especially sensitive to age-dependent changes in the LVCP secretome
- Transcriptome analysis reveals novel facets of LVCP biology

### Accession Numbers

GSE82308



# Age-Dependent Niche Signals from the Choroid Plexus Regulate Adult Neural Stem Cells

Violeta Silva-Vargas,<sup>1,2</sup> Angel R. Maldonado-Soto,<sup>3</sup> Dogukan Mizrak,<sup>2</sup> Paolo Codega,<sup>2,4</sup> and Fiona Doetsch<sup>1,2,3,5,\*</sup>

<sup>1</sup>Biozentrum, University of Basel, 4056 Basel, Switzerland

<sup>2</sup>Department of Pathology and Cell Biology, Columbia University, New York, NY 10032, USA

<sup>3</sup>Department of Neuroscience, Columbia University, New York, NY 10032, USA

<sup>4</sup>Present address: Memorial Sloan Kettering Cancer Center, New York, NY 10065, USA

<sup>5</sup>Lead Contact

\*Correspondence: [fiona.doetsch@unibas.ch](mailto:fiona.doetsch@unibas.ch)

<http://dx.doi.org/10.1016/j.stem.2016.06.013>

## SUMMARY

Specialized niches support the lifelong maintenance and function of tissue-specific stem cells. Adult neural stem cells in the ventricular-subventricular zone (V-SVZ) contact the cerebrospinal fluid (CSF), which flows through the lateral ventricles. A largely ignored component of the V-SVZ stem cell niche is the lateral ventricle choroid plexus (LVCP), a primary producer of CSF. Here we show that the LVCP, in addition to performing important homeostatic support functions, secretes factors that promote colony formation and proliferation of purified quiescent and activated V-SVZ stem cells and transit-amplifying cells. The functional effect of the LVCP secretome changes throughout the lifespan, with activated neural stem cells being especially sensitive to age-related changes. Transcriptome analysis identified multiple factors that recruit colony formation and highlights novel facets of LVCP function. Thus, the LVCP is a key niche compartment that translates physiological changes into molecular signals directly affecting neural stem cell behavior.

## INTRODUCTION

Stem cells reside in specialized niches that support their lifelong maintenance. Stem cell niches undergo dynamic changes in response to different physiological states, including aging; however, little is known about how these extrinsic changes affect stem cell behavior. In the adult mouse brain, the ventricular-subventricular zone (V-SVZ), adjacent to the lateral ventricles, harbors neural stem cells (NSCs) that give rise to olfactory bulb neurons as well as astrocytes and oligodendrocytes throughout life (Figure 1A). V-SVZ stem cells are specialized glial fibrillary acidic protein (GFAP)-positive radial astrocytes that extend a short apical process to contact the cerebrospinal fluid (CSF), which circulates through the brain ventricular system (Figure 1A), and a long basal process that terminates on blood vessels (reviewed in Fuentealba et al., 2012) (Figure 2A). The vascular niche is an important mediator of proliferation in the adult V-SVZ (reviewed

in Silva-Vargas et al., 2013); however, the role of the CSF compartment in regulating adult NSCs is just beginning to be explored.

The CSF provides important homeostatic support for the brain (Redzic et al., 2005). The CSF milieu is complex, contains active signaling cues from local and long-range sources (Johansson, 2014), and changes over the lifespan (Baird et al., 2012; Chen et al., 2012). The CSF is emerging as an important player in brain morphogenesis and proliferation during brain development (Johansson, 2014; Lehtinen et al., 2011). In the adult, the CSF compartment provides migratory cues for newly generated neurons (Sawamoto et al., 2006) and contains factors that actively maintain stem cell quiescence (Codega et al., 2014; Kokovay et al., 2012; Delgado et al., 2014).

The CSF is primarily produced by the choroid plexus (CP), a vascularized epithelial structure floating within the brain ventricles that constitutes the blood-CSF barrier (Figures 1A, 2A, and S1A). In addition to its important role in brain homeostasis, including the production of bulk CSF fluid (Redzic et al., 2005), the CP actively synthesizes and secretes diverse signaling factors (Lun et al., 2015). A less-appreciated facet of the CP is that it acts as a sensor, integrating and dynamically responding to physiological signals from the circulation, nervous system, and immune system (Baruch et al., 2014; Marques and Sousa, 2015; Strazielle et al., 2016).

As such, it is important to specifically illuminate how the lateral ventricle CP (LVCP), with its close proximity to the V-SVZ, affects cell dynamics within the niche under different states, including aging. Here we show that the LVCP is a key novel component of the adult V-SVZ NSC niche, differentially affecting the behavior of multiple cell types.

## RESULTS

### LVCP-Secreted Factors Support the Proliferation of V-SVZ Cells

To directly investigate how the LVCP secretome regulates adult V-SVZ NSCs and their progeny, we set up a simple system to harvest conditioned medium from LVCP explants (LVCPsec) (Figure S1B). Bulk V-SVZ cells cultured with LVCPsec, without any additional growth factors, promoted the formation and proliferation of multipotent neurospheres (Figures 1B and 1C). This effect was due to LVCPsec and not factors present in blood, which also can affect SVZ proliferation (Katsimpardi

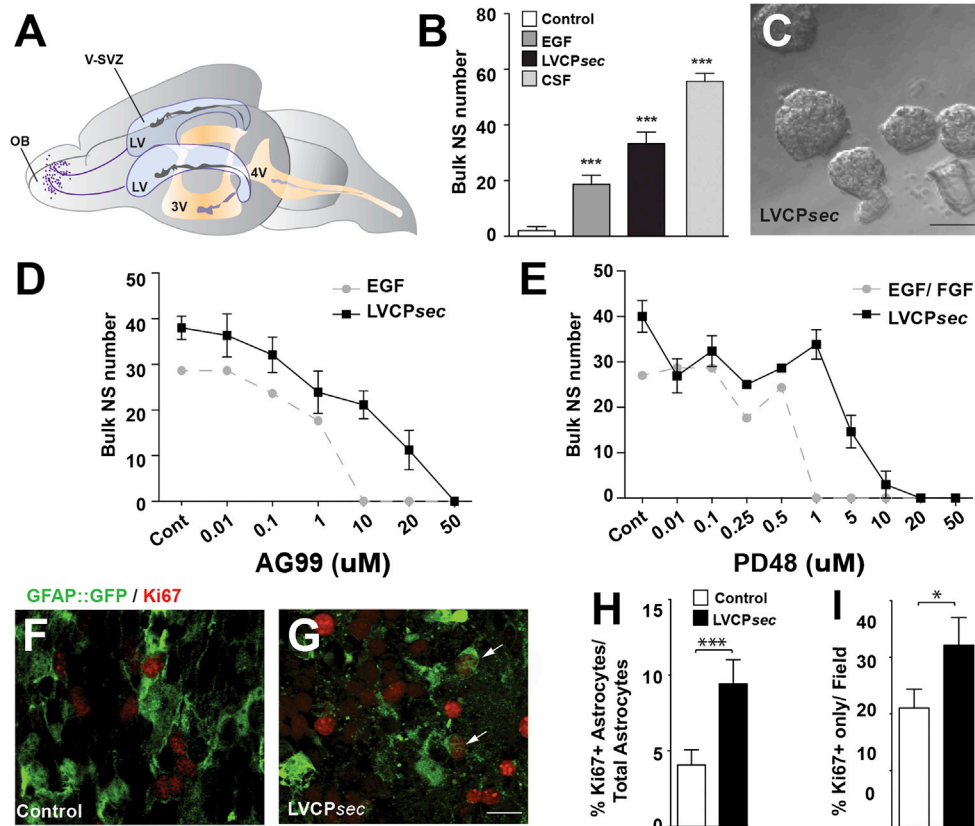


### Figure 1. CP-Secreted Factors Induce Proliferation of V-SVZ Cells

(A) Schema showing ventricular system of adult mouse brain and V-SVZ stem cell niche (light blue) along length of lateral ventricle (LV). Newly generated neurons (purple) migrate to the olfactory bulb (OB). The CSF flows unidirectionally from the LV into the third (3V) and then into the fourth ventricle (4V) where it is reabsorbed into circulation. CP (dark gray structures) are present in each brain ventricle.

(B) Quantification of neurospheres (NS) formed by bulk SVZ cells. Data represent mean number of NS formed in each condition  $\pm$  SEM ( $n = 3$ ; one-way ANOVA with Bonferroni correction,  $p < 0.0001$ ).

(C) Differential interference contrast (DIC) image shows NS formed with LVCPsec.

(D) NS formation with LVCPsec or EGF in the presence of AG99 is shown.

(E) NS formation with LVCPsec or EGF/bFGF in the presence of PD48 is shown.

(F and G) Confocal images of SVZ whole mounts of control (F) or LVCPsec- (G) infused GFAP::GFP brains immunostained for Ki67 and GFP. Arrows in (G) show double-labeled cells.

(H and I) Percentages of dividing V-SVZ astrocytes (Ki67+GFP+) (H) and of other dividing V-SVZ cells (GFP-Ki67+) (I). Data represent mean percentage of proliferating cells  $\pm$  SEM ( $n = 3$ ; \* $p < 0.05$  and \*\*\* $p < 0.001$ , Student's  $t$  test).

Scale bars, 85  $\mu$ m (C) and 15  $\mu$ m (G). See also Figure S1.

et al., 2014), as no difference was observed when mice were perfused with saline to remove blood prior to LVCP explantation (Figure S1C).

Notably, both LVCPsec and freshly isolated CSF from the cisterna magna promoted the formation of significantly more, but smaller, neurospheres than the epidermal growth factor (EGF)-only condition (Figure 1B), suggesting that factors present in this compartment other than EGF also are involved. Indeed, pharmacological inhibition of canonical V-SVZ-signaling pathways showed that 60% of neurospheres still formed with AG99 (EGF receptor [EGFR] inhibitor) and 75% with PD48 (CAS 1135256-66-4, EGF/fibroblast growth factor [FGF]/platelet-derived growth factor [PDGF] receptor tyrosine kinase inhibitor) (Figures 1D and 1E) at inhibitor concentrations where no neurospheres formed in the controls. To assess if factors secreted by the LVCP also affect V-SVZ cells in vivo, concentrated LVCPsec

was infused into the lateral ventricles of adult GFAP::GFP mice for 6 days, and whole mounts were immunostained for Ki67, a marker of cell division. Infusion resulted in a 2-fold increase in GFAP::GFP+Ki67+ V-SVZ astrocytes and a 1.5-fold increase in dividing GFAP::GFP-Ki67+ progenitors (Figures 1F–1I), suggesting that LVCPsec regulates multiple populations of V-SVZ cells.

### LVCP-Secreted Factors Support Clonal Proliferation of qNSCs, aNSCs, and TACs

To precisely define which V-SVZ populations respond to LVCP signals, we used fluorescence-activated cell sorting (FACS) to isolate cells from each stage of the lineage. FACS-purified quiescent NSCs (qNSCs, GFAP::GFP<sup>+</sup>CD133<sup>+</sup>EGFR<sup>-</sup>CD24<sup>-</sup>), activated NSCs (aNSCs, GFAP::GFP<sup>+</sup>CD133<sup>+</sup>EGFR<sup>+</sup>CD24<sup>-</sup>), transit-amplifying cells (TACs, GFAP::GFP<sup>-</sup>CD133<sup>-</sup>EGFR<sup>+</sup>CD24<sup>-</sup>), and neuroblasts (GFAP::GFP<sup>-</sup>CD133<sup>-</sup>EGFR<sup>-</sup>CD24<sup>+</sup>)

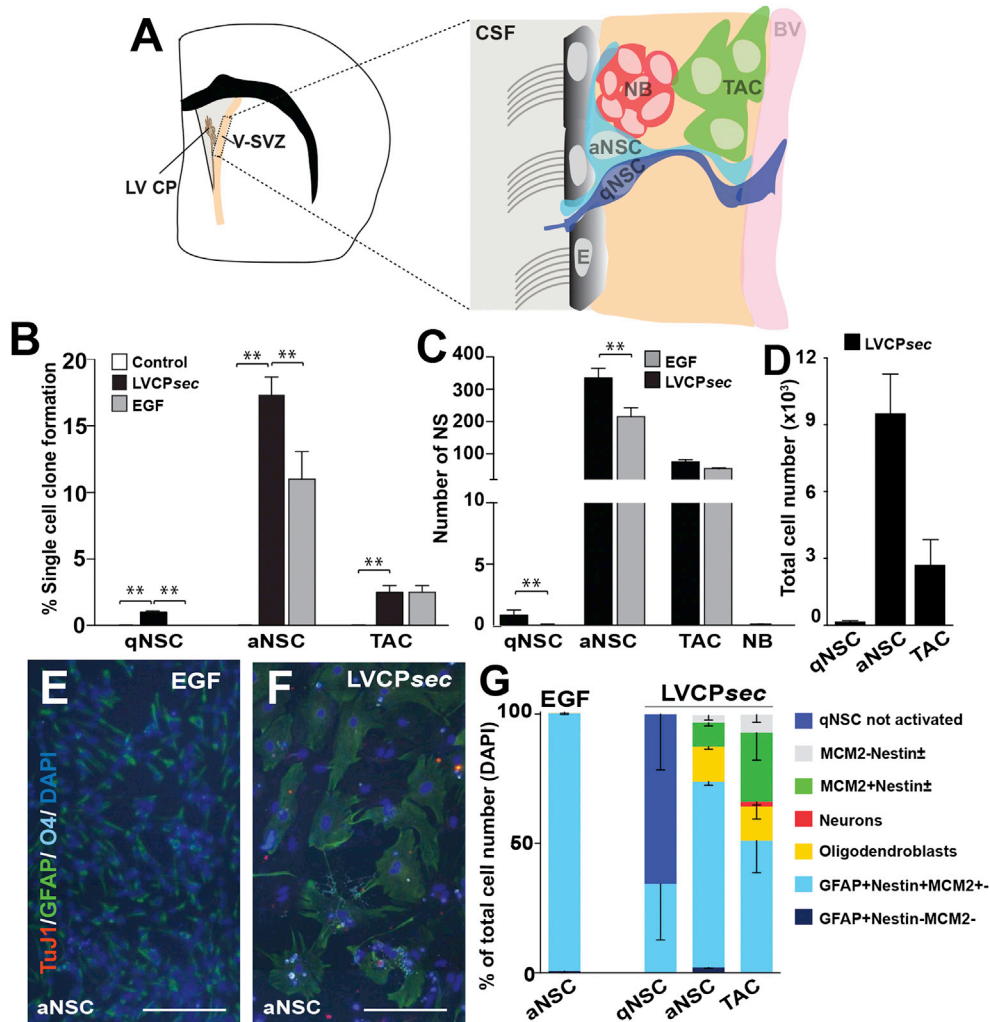


**Figure 2. LVCP-Secreted Factors Support Clonal Proliferation of qNSCs, aNSCs, and TACs**

(A) Schema of coronal brain section showing V-SVZ adjacent to the CSF-filled lateral ventricles. The LVCP floats in the LV in close proximity to the V-SVZ. Box is expanded to right showing V-SVZ cell types. Quiescent neural stem cells (qNSC) are radial cells contacting both the CSF and blood vessels (BV). The qNSCs become activated (aNSC) and in turn give rise to transit-amplifying cells (TAC) that generate neuroblasts (NB). Multi-ciliated ependymal cells (E) line the ventricles.

(B) Quantification of single-cell-adherent colony formation by FACS purified V-SVZ populations. Data represent mean percentage of single-cell clones formed  $\pm$  SEM (n = 3; one-way ANOVA with Bonferroni correction,  $p < 0.0001$ ).

(C) Quantification of primary NS formed by FACS-purified V-SVZ populations. Data represent mean NS number formed  $\pm$  SEM (n = 3; \*\* $p < 0.01$ , Student's t test). See also [Figures S1E–S1G](#) and [S1I–S1N](#).

(D) Quantification of total cell number (DAPI+) after 14 days of adherent culture of FACS-purified cells with LVCPsec. Data represent the mean of each population for the entire well  $\pm$  SEM (n = 6). No population proliferated in control unconditioned medium. See also [Figure S1H](#).

(E and F) Representative images show aNSCs cultured with EGF only (E) or LVCPsec (F) for 14 days and immunostained for TuJ1, O4, and GFAP. Scale bar, 100  $\mu$ m.

(G) Quantification of different cell types after culture with LVCPsec for 14 days. Data represent the mean of each population  $\pm$  SEM (n = 3).

(Codega et al., 2014; Pastrana et al., 2009) ([Figures 2A](#) and [S1D](#)) were cultured with LVCPsec, without exogenous growth factors, under either adherent colony formation or neurosphere conditions.

LVCPsec alone promoted both the recruitment ([Figures 2B](#) and [2C](#)) and division ([Figures 2D](#) and [S1H](#)) of single qNSCs, aNSCs, and TACs to form adherent colonies, as well as self-renewing neurospheres that were multipotent and gave rise to neurons, astrocytes, and oligodendrocytes upon differentiation ([Figures](#)

[S1E–S1G](#) and [S1I–S1M](#)), with significantly greater neuronal and oligodendrocyte differentiation than EGF only ([Figure S1N](#)). Notably, LVCPsec recruited a significantly greater number of qNSCs and aNSCs to divide in both assays than the EGF-only condition ([Figures 2B](#) and [2C](#)), but the individual colonies were smaller ([Figures S1E–S1G](#); data not shown). LVCPsec-adherent cultures of qNSCs, aNSCs, and TACs were also far more heterogeneous than EGF-only conditions, which contained relatively homogeneous GFAP+Nestin+ spindle-shaped cells,

after 14 days (Figures 2E and 2F). All LVCPsec cultures contained predominantly GFAP+Nestin+ progenitors with different morphologies. Strikingly, both aNSCs and TACs also gave rise to a unique expansion of the oligodendrocyte lineage (15%–20% of culture) (Figure 2G). TACs also generated a large number of MCM2+GFAP– progenitors. In addition, some mature neurons were present in aNSC and TAC cultures. The LVCP therefore provides a diverse repertoire of factors that affect multiple populations in the adult V-SVZ with cell-type-specific effects.

### V-SVZ Cells Differentially Sense Aging-Related Changes in the LVCP Secretome

The LVCP dynamically alters its secretome in response to changes in physiological states (Baruch et al., 2014; Redzic et al., 2005). We therefore investigated whether aging, a physiological state that greatly impacts stem cell behavior, alters the functional effect of LVCPsec. In vivo, levels of adult V-SVZ proliferation and neurogenesis decrease dramatically with aging (reviewed in Conover and Shook, 2011 and Signer and Morrison, 2013). This decline is due to both intrinsic changes in the stem cells/progenitors and to extrinsic modifications in the niche, including systemic changes in circulating factors (Bouab et al., 2011; Katsimpardi et al., 2014; Piccin et al., 2014).

We first compared the intrinsic capacity of FACS-purified V-SVZ populations from young (2-month-old) and aged (>18-month-old) mice to respond to EGF. The total number of qNSCs, aNSCs, and TACs obtained per mouse was significantly reduced in aged mice (Figure S2A). Despite their lower number, aNSCs and TACs from aged mice did not exhibit significant differences in the frequency of colony formation in response to EGF in either single-cell-adherent conditions or in the neurosphere assay compared to young mice (Figures S2B and S2C). In contrast, aged qNSCs exhibited a significant decrease in the percentage of colonies formed as compared to young qNSCs (Figures S2B and S2C); however, those neurospheres that formed from old qNSCs could be serially passaged (Figure S2C). Thus, the extrinsic niche plays an important role in aging-related decreases in proliferation in vivo.

To directly assess how aging alters the functional effect of the LVCP secretome on the adult V-SVZ, we cultured FACS-purified cells from young and aged mice with either age-matched or heterochronic LVCPsec (Figure 3A). Strikingly, aNSCs were especially sensitive to aging-related changes in the LVCP secretome, with young aNSCs showing a decrease by almost one-half in clone recruitment when cultured with aged LVCPsec (Figure 3B). Conversely, higher numbers of aged aNSCs were recruited to form clones in the presence of young LVCPsec. In contrast, neither qNSCs nor TACs exhibited significant changes in clone recruitment in response to heterochronic LVCPsec. As factors in the circulation can impact the V-SVZ during aging (Katsimpardi et al., 2014), we confirmed that the heterochronic effects we observed were due to LVCPsec and not factors present in blood. No difference was observed when mice were perfused with saline to remove blood prior to LVCP explantation (Figure S2D).

To evaluate the age-dependent effect of the CP secretome in vivo, we cross-infused LVCPsec from aged mice into young GFAP::GFP transgenic mice, and vice versa (Figure 3C), and quantified proliferation by immunostaining for MCM2 and

GFP in whole-mount preparations. Infusion of aged LVCPsec resulted in a significant decrease in MCM2+ GFAP::GFP+ V-SVZ astrocytes, but not of MCM2+ GFAP::GFP-negative progenitors in the V-SVZ (Figure 3D). Conversely, heterochronic infusion of young LVCPsec into aged mice led to a significant increase only in the number of MCM2+ GFAP::GFP+ V-SVZ astrocytes. Together these results show that NSCs are especially sensitive to age-dependent changes in the LVCP secretome.

### Multiple Aspects of aNSC Behavior Are Sensitive to Age-Dependent Changes in LVCPsec

To directly probe how age-dependent changes in LVCPsec affect aNSC behavior, we cultured FACS-purified aNSCs with age-matched or heterochronic LVCPsec for 14 days (Figure 3F), and we analyzed proliferation, progenitor, and differentiation status. In heterochronic LVCPsec cultures, young cells exhibited an ~50% decrease in MCM2+ cells upon exposure to old LVCPsec. Conversely, while old cells cultured with old LVCPsec had almost no MCM2+ cells, exposure to young LVCPsec increased MCM2+ cells to 22% (Figures 3H and S3A). The age-related LVCPsec-induced changes in MCM2 did not result in significant changes in the total cell number generated by young or old aNSCs, although overall young aNSCs generated more cells than old aNSCs (Figure S3B).

Heterochronic cultures also affected progenitor and differentiation status (Figures 3G, 3H, and S3C–S3H). Old aNSCs cultured with old LVCPsec had a reduction in GFAP+Nestin+ and Nestin+MCM2+ cells, with a concomitant increase in Nestin+MCM2– large flat cells and Nestin+MCM2– small cells as compared to young aNSCs cultured with young LVCPsec (Figures 3H, S3H, S3I, and S3L). Moreover, dividing aNSCs (Figures 3H, S3H, and S3J), radial GFAP+Nestin– quiescent cells, and GFAP+Nestin– stellate cells were almost completely absent in old-old cultures (Figures 3H, S3H, S3K, and S3M). Strikingly, heterochronic culture of old aNSCs with young LVCPsec reversed the decrease in dividing aNSCs and Nestin+MCM2+ cells, as well as the increase in both Nestin+MCM2– large flat cells and Nestin+MCM2– small cells (Figures 3H, S3H, S3I, and S3J). It also resulted in a 2.5-fold increase of both small round TuJ1+ neuroblasts and neurons (Figures 3G, 3H, and S3H). Young aNSCs also were affected by culture with old LVCPsec, with fewer dividing aNSCs and Nestin+MCM2+ cells (Figures 3H, S3H, and S3J). In contrast, the proportion of oligodendroblasts did not change significantly with aging or with heterochronic culture (Figures 3G, 3H, and S3H). Thus, age-related changes in LVCPsec affect proliferation, progenitor, and differentiation status of aNSCs.

### Transcriptome Analysis Reveals Novel LVCP Factors

Together, our functional experiments show that the LVCP is a dynamic niche compartment with multiple effects on V-SVZ stem cells and their progeny. To gain insight into the repertoire of secreted signals in LVCPsec, we performed transcriptome analysis of young (2-month-old) and aged (18-month-old) LVCP (Figure 4A). Global analysis of all LVCP-expressed probesets with MetaCore confirmed the role of LVCP in homeostatic and barrier functions, but also revealed less-explored processes related to nervous system development, cell cycle, oligodendrocyte

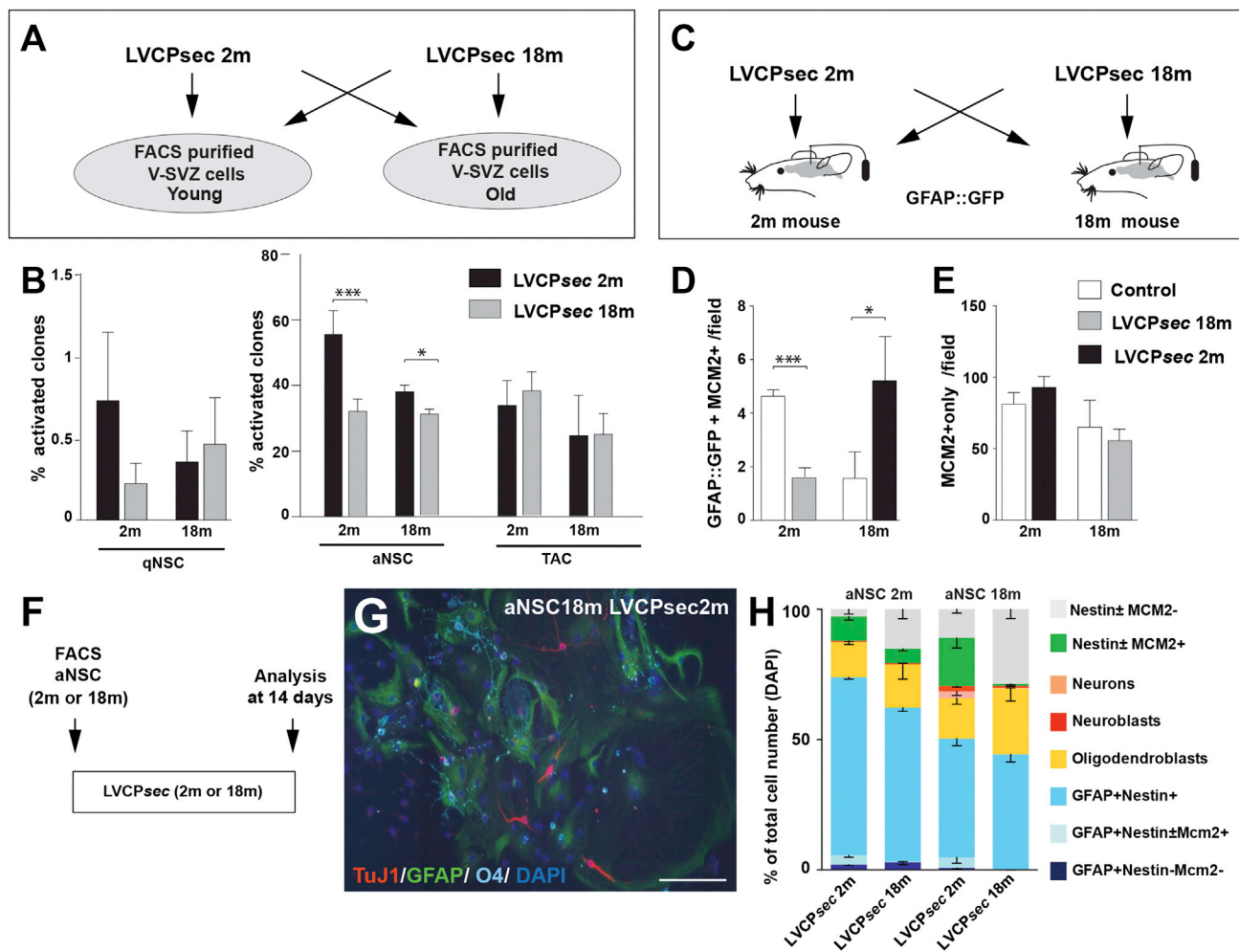


**Figure 3. Age-Dependent Effect of LVCPsec on V-SVZ Cells**

(A) Schema shows experimental design to determine functional effect of aging on LVCPsec in vitro. (B) Quantification of clone formation by purified qNSCs, aNSCs, and TACs from young and old mice with young and old LVCPsec. Data represent mean percentage of clone formation by each population  $\pm$  SEM (n = 9; one-way ANOVA with Bonferroni correction,  $p < 0.0001$ ). See also Figure S2. (C) Schema shows experimental design to determine functional effect of aging on LVCPsec in vivo. (D and E) Quantification of MCM2+GFAP::GFP+ V-SVZ astrocytes (D) and MCM2+GFAP::GFP-negative SVZ cells (E) (one-way ANOVA analysis with Bonferroni correction with either age,  $p < 0.01$  in mice infused with young or old LVCPsec or control unconditioned media). Data represent the mean number of cells per field  $\pm$  SEM (n = 6). (F) Schema of experimental design to determine functional effect of aging on LVCPsec on aNSCs in vitro. 100 FACS-purified aNSCs from young and old mice were cultured with young (2-month-old) or old (>18-month-old) LVCPsec for 14 days. (G) Representative image shows 18-month-old aNSCs cultured with 2-month-old LVCPsec and immunostained for TuJ1, O4, and GFAP. Scale bar, 100  $\mu$ m. (H) Quantification of different cell types present in cultures after 14 days. See also Figure S3. Data represent the mean of each population  $\pm$  SEM (n = 3). For each cell type two-way ANOVA analysis with Bonferroni correction was performed (aNSC 2 months with aNSC 18 months: GFAP+Nestin+  $p < 0.037$ ; aNSC 18 months LVCPsec 18 months comparison with aNSC 18 months LVCPsec 2 months: NBs  $p < 0.046$ , neurons  $p < 0.018$ , and Nestin  $\pm$  MCM2-  $p < 0.0009$ ; and aNSC 18 months LVCPsec 18 months comparison with aNSC 2 months LVCPsec 2 months: Nestin  $\pm$  MCM2+  $p < 0.032$ ). For statistics of GFAP+Nestin+MCM2+ cells, see Figure S3.

differentiation, axonal transport, and multiple signaling pathways (Figures S4A and S4B; Table S1). Strikingly, analysis of LVCP-enriched genes compared to qNSC and aNSC populations (see the Experimental Procedures) with the disease biomarker enrichment tool revealed that the top ten disease categories were all CNS or metabolic related (Figure 4B; Table S1), underscoring the emerging importance of the LVCP for disease (Marques and Sousa, 2015). Moreover, glucuronidation-related processes implicated in drug metabolism and xenobiotic protec-

tion (Ouzzine et al., 2014) were most enriched in young mice (Figure S4H). In contrast, in aged mice categories related to immune response, inflammation, and interferon gamma were enriched (Figure S4H), as previously described (Baruch et al., 2014). This analysis highlights the complexity and multiple functions of the LVCP in health and disease.

Our findings show that LVCPsec contains novel factors that promote greater clone recruitment than EGF/basic FGF (bFGF) alone (Figure 1). To screen for novel candidates, we combined

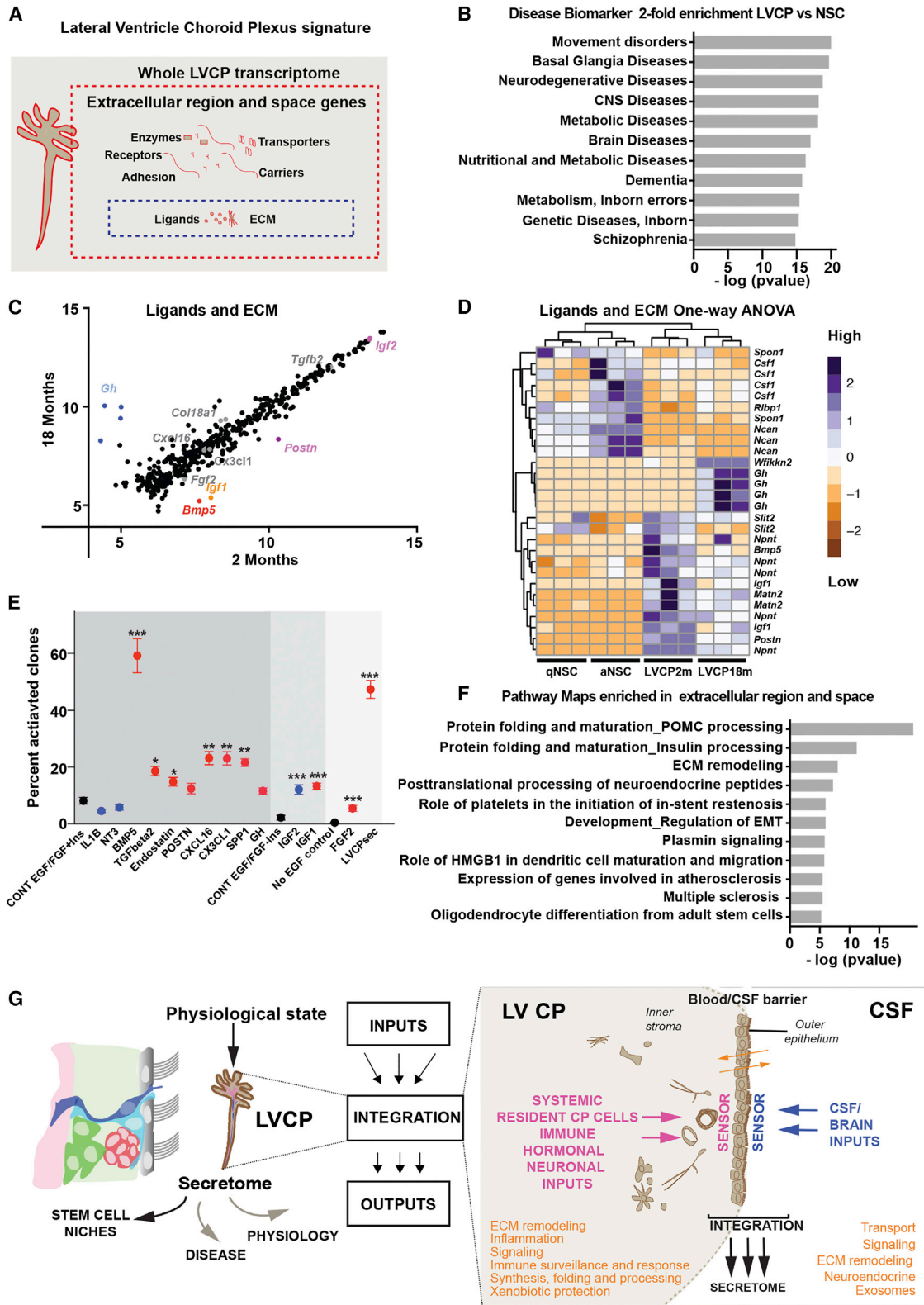


**Figure 4. Transcriptome Analysis Identifies Novel Factors and Facets of LVCP Function**

(A) Outline of strategy for transcriptome analysis of whole LVCP. Whole-LVCP transcriptome was analyzed to illuminate CP function, extracellular region, and extracellular space genes to define secretome-related processes (red box) and ligands and ECM genes for the candidate screen (blue box).

(legend continued on next page)

transcriptome analysis of whole LVCP and proteomic analysis of LVCPsec. To identify secreted candidate genes, we applied gene ontology (GO) cellular component filters for extracellular space and extracellular region, which include enzymes, transmembrane receptors, transporters, adhesion molecules, carriers, ligands, and extracellular matrix (ECM) (Figure 4A). We then manually curated a list of ligands and ECM molecules (Figures 4A and 4C; Table S1). Many were present (447 probesets) and only a few showed age-dependent changes (Figures 4C, 4D, and S4G; Table S1). Hierarchical clustering of differentially expressed ligands and ECM genes from the comparison of LVCP with qNSC and aNSC populations revealed unique LVCP clusters and others shared with qNSCs and aNSCs (Figure 4D).

Proteomic analysis by antibody arrays confirmed that LVCPsec contains multiple novel ligands and ECM-related factors, including chemokines and lymphokines (CSF-1, CCL2/JE, CXCL16, CX3CL1, and CXCL12), growth factors (TGFbeta2, FGF2, PLGF, LIF, and VEGF-A), carriers (Fetuin-A and RBP4), enzymes (PD-ECGF), hormones (Adiponectin), and ECM and ECM remodelers (Endocan, SPP1, SERPINE1, MMP-3, MMP-8, and TIMP-1), as well as previously reported LVCP-derived factors (IGFBP-2, IGFBP-3, IGF2, Lipocalin-2, and IL1B) (Figure S4E). Some of these proteins (FGF2, PLGF, CXCL12, LIF, and VEGF-A) already have been implicated in the regulation of V-SVZ cells, revealing that the LVCP is an additional source of these factors. Notably, many of the genes for these proteins are enriched in LVCP as compared to qNSCs and aNSCs (Figure S4F).

Using our transcriptome and proteomic data, we selected a pool of novel candidates to functionally test for their ability to induce clone recruitment. As aged LVCPsec dramatically decreased clone recruitment from young cells, we tested factors that changed with aging and some that did not (Figures 4E and S4G). We confirmed that IL1B and NT-3 both decreased the number of clones recruited, whereas IGF2 promoted clone formation (Delgado et al., 2014; Kokovay et al., 2012; Lehtinen et al., 2011). Strikingly, we identified two novel candidates, BMP5 and IGF1, both enriched in young LVCP, which had potent effects on clone recruitment over their controls. BMP5 stimulated clone recruitment to 60%, similar to LVCPsec. In addition, TGFbeta2, Endostatin, CXCL16, CX3CL1, and SPP1 also promoted recruitment of colony formation over EGF/bFGF baseline

levels. Thus, the LVCP secretome contains a reservoir of diverse factors that can promote quiescence as well as activation and proliferation of V-SVZ cells.

To get more insight into the role of the LVCP in the niche, we analyzed all genes in extracellular region and space filters (Figure 4A). Unexpectedly, the top enriched pathway maps included neuropeptide and hormone synthesis, processing and post-translational modifications (POMC, insulin, and neuroendocrine peptides), oligodendrocyte differentiation from stem cells, and multiple sclerosis (Figure 4F), highlighting an important role for neuropeptide and hormonal modulation, and supporting our functional data showing that LVCPsec promotes the oligodendrocyte lineage in V-SVZ. Categorization of all the biologically relevant processes and networks that were significantly enriched (Figures 4F, S4C, and S4D; Table S1) revealed unexpected and diverse aspects of LVCP niche functions, including ECM remodeling, immune modulation and inflammation, activation and inhibition of numerous signaling pathways, metabolism, multiple catalytic activities, protein processing and modification, cell trafficking, differentiation (neurogenesis and gliogenesis), and proliferation. Strikingly, ~20% of the GO categories were related to cell sensing and response to diverse stimuli (Figure S4C; Table S1). Together our analysis highlights novel dimensions of LVCP function, including that of a stem cell niche compartment, which dynamically senses the environment and is a source of diverse secreted factors that modulate V-SVZ cells (Figure 4G).

## DISCUSSION

Here we uncover a novel role for the LVCP as a key component of the adult V-SVZ niche. In addition to maintaining quiescence, secreted factors from the LVCP directly regulate multiple aspects of the behavior of adult V-SVZ stem cells and their progeny. Moreover, the functional effect of the LVCP secretome changes with aging, with NSCs being especially sensitive to aging-related changes. Our transcriptome and proteomic analyses identified novel candidates and revealed unexpected facets of LVCP function. Together our findings uncover the LVCP as an important niche compartment that dynamically contributes to age-related changes in the V-SVZ.

The CP is a complex structure with specialized epithelial cells and a vascularized and innervated stroma containing diverse cell

(B) Disease biomarker enrichment analysis for significantly enriched LVCP genes compared to V-SVZ NSCs. The input gene list (3,543 probesets) represents the overlap of LVCP-enriched genes as compared to qNSC and aNSC populations ( $p < 0.05$ ). See also Table S1.

(C) Scatterplot of 2-month versus 18-month LVCP-expressed ligands and ECM genes (447 probesets). The values represent  $\log_2$ -transformed expression levels. The genes screened for clone formation efficiency are highlighted in color. See also Table S1.

(D) Hierarchical clustering of significantly different LVCP ligands and ECM genes from comparison of qNSC, aNSC, 2-month, and 18-month LVCP samples ( $p \leq 0.05$ , one-way ANOVA). Color map values are assigned based on the SD from the row mean. The 2-month-enriched LVCP factors include *Slit2*, *Npnt*, *Bmp5*, *Igf1*, *Matn2*, and *Postn*, and the 18-month-enriched factors include *Wfikkn2* and *Gh*.

(E) Ligand screen of LVCP candidates. Quantification of NS clone recruitment with previously tested factors IL1B, NT3, and IGF2 (blue) and novel factors BMP5, TGFbeta2, Endostatin, POSTN, CXCL16, CX3CL1, SPP1, GH, IGF1, and FGF2 (red). Dark gray background indicates control medium containing Insulin, medium gray indicates no Insulin, and light gray indicates no growth factors. Data represent the mean of each condition and the error bars indicate SEM (one-way ANOVA with Bonferroni correction was performed,  $p$  value summary  $p < 0.0001$ ; enriched in 2-month LVCP: *Bmp5*, *Igf1*, and *Postn*; enriched in 18-month LVCP: *Il1b*, *Gh*, and *Col18a1* [endostatin]). Factors that did not exhibit age-dependent changes but were present in our proteomics analysis were IGF2, CX3CL1, CXCL16, FGF2, NT3, and TGFbeta2 (Figures 4C and 4D; see also Figures S4E–S4G).

(F) Pathway enrichment analysis for all extracellular region and space LVCP genes (991 probesets). The probeset list was imported into MetaCore to investigate overrepresented pathways within the dataset ( $p < 0.01$ , false discovery rate [FDR]  $< 0.01$ ). The  $p$  values are calculated based on hypergeometric distribution, and FDR adjustment was applied to avoid false positives. Resulting pathways were ranked by  $-\log(p$  value). The top 11 pathways are shown. The top 50 are given in Table S1.

(G) Schema highlights multiple functions of the LVCP.

types, including immune cells, microglia, fibroblasts, and macrophages (Figure 4G), which all contribute to the LVCP secretome. Previous CP studies have defined the physical, enzymatic, and neuroimmunological properties of this barrier, revealing its essential secretory and regulatory functions for physiological brain homeostasis, role in immunosurveillance and inflammatory and repair processes, and emerging contribution to neuropsychiatric and neurodegenerative disease. Our findings now link LVCP secretome with the modulation of stem cell dynamics in the adult V-SVZ, highlighting that the LVCP also acts as a stem cell niche compartment.

LVCPsec differentially regulates multiple aspects of qNSC, aNSC, and TAC behavior, affecting both cells that directly contact the CSF and those that do not. Culture with LVCPsec recapitulates more of the *in vivo* complexity and supports the expansion of diverse lineages from purified V-SVZ cell populations. Cells are found at multiple stages in these complex cultures. While most are maintained as progenitors, including a substantial fraction of oligodendroblasts, also differentiated neurons, oligodendrocytes, and astrocytes are present.

LVCPsec promotes the recruitment of more qNSC and aNSC clones than EGF only, suggesting that additional pools of V-SVZ stem cells are differentially recruited and supported by LVCPsec. From our screen, we identify several novel ligands that promote the recruitment of colony formation over EGF/bFGF baseline levels. Notably, BMP5 resulted in a dramatic increase in the number of clones recruited, similar to its effect on epidermal stem cell recruitment (Kangsamaksin and Morris, 2011). IGF1 also promoted clone recruitment over baseline levels. Whether the expansion of the oligodendrocyte lineage with LVCPsec as compared to EGF-only cultures is due to the *de novo* recruitment of oligodendrocyte-committed progenitors and/or a richer repertoire of signals that supports the generation of oligodendroblasts from stem cells needs to be further explored. Notably, oligodendrocyte differentiation from adult stem cells and multiple sclerosis are two of the most enriched categories in our transcriptome analysis. As such, the CP may be a key source of secreted signals that mediate oligodendrocyte production. Indeed, Wnts are present in the CSF (Lehtinen et al., 2011) and support oligodendrogenesis (Azim et al., 2014; Ortega et al., 2013). The greater recruitment of NSCs to form colonies by LVCPsec suggests that NSC heterogeneity in part reflects distinct pools of NSCs, perhaps with different functions, that respond to unique combinations of signals. In the future, it will be important to dissect how diverse LVCP niche cues differentially affect V-SVZ cell types, whether LVCP factors contribute to regional stem cell identity, and how they impact cell dynamics and lineage in this stem cell compartment.

The aging CP undergoes important changes modifying both its transcriptome and secretory capacity (our data; Baruch et al., 2014; Redzic et al., 2005). Intriguingly, not all V-SVZ cell types were sensitive to changes in the aged LVCP secretome, with aNSCs, but not TACs, being affected. Aged aNSCs divide extensively with EGF only. In contrast they exhibit very different behavior with aged LVCPsec, including a shift in progenitor status, loss of cycling aNSCs, and the appearance of Nestin+MCM2– large flat cells, which may be the first signs of senescence. Some of these changes are reversed by exposure

to young LVCPsec. Interestingly, two of the candidates we identified, BMP5 and IGF1, are enriched in young LVCP. BMP5 levels are lower in aged human CSF than in young (Baird et al., 2012), and systemic levels of IGF1 also decrease with aging in rodents and humans (Bartke et al., 2013), suggesting that BMP5 and IGF1 may be important factors in the age-dependent recruitment effect of the LVCP secretome on V-SVZ stem cells. Levels of Slit2, which is important for neuroblast migration (Sawamoto et al., 2006), also decrease in aging LVCP, and they also may contribute to the decline in neurogenesis *in vivo* with aging. Together, our findings highlight that the LVCP is an important contributor to extrinsic changes during aging, adding to the growing number of niche compartments affected by aging (Katsimpardi et al., 2014; Piccin et al., 2014). In the future it will be important to see how other physiological states dynamically affect the LVCP niche compartment.

Importantly, with its unique location at the interface between the blood and the CSF, the CP itself can sense and respond to local changes in the niche as well as to different physiological signals by changing its secretome (reviewed in Marques and Sousa, 2015; Figure 4G). Indeed, CP epithelial cells express an array of growth factor and hormone receptors, allowing them to sense changes in different states (our data; Marques et al., 2011). Interestingly, our transcriptome analysis revealed that hormones and neuropeptides, not previously associated with LVCP, might be actively processed by the CP, including hormones from the somatotrophic axis, such as GH and IGF1, that exhibit age-dependent patterns. The LVCP is therefore positioned to be a key component of metabolic and neuroendocrine regulation (Figure 4G), potentially having a long-range effect on global physiology and pathological states.

With its unique position receiving inputs from the circulatory, autonomic, and immune systems, the LVCP is poised to act as a key regulatory hub, integrating local and long-range signals from different parts of the body and dynamically modulating its contribution to the V-SVZ stem cell niche (Figure 4G). Elucidating the functional regulation and output of the LVCP will provide insight into adult NSC behavior, how it can be modulated in health and disease, and eventually harnessed for brain repair.

## EXPERIMENTAL PROCEDURES

All experiments were performed in accordance with institutional and national guidelines for animal use.

### Preparation of LVCPsec and CSF Collection

Details of the preparation of LVCPsec and CSF isolation from the cisterna magna are provided in the [Supplemental Experimental Procedures](#).

### FACS Purification

V-SVZ cells were FACS purified from GFAP::GFP mice (Jackson Laboratory) as previously described (Codega et al., 2014; Pastrana et al., 2009).

### Analysis and Quantification

Statistical analysis was performed using Prism 6. Two-way comparisons were performed using a Student's *t* test. When comparing more than two datasets, ANOVA analysis was used to determine significance followed by the Bonferroni multiple comparison test on pairwise comparisons.

### In Vitro Culture

All LVCPsec experiments were done without any additional growth factors in the medium. See the [Supplemental Experimental Procedures](#) for details of assays.

### In Vivo Infusion

LVCPsec was infused into the lateral ventricles of GFAP::GFP mice for 6 days with a mini-osmotic pump (Alzet 1007D). See the [Supplemental Experimental Procedures](#) for details.

### Immunostaining

Cells were fixed and immunostained as described in the [Supplemental Experimental Procedures](#).

### LVCP RNA Isolation and Microarray Hybridization

The mRNA was purified from 2- or 18-month-old LVCP of CD1 mice. The cDNA was synthesized and hybridized to Affymetrix Mouse Genome 430 2.0 Arrays. See the [Supplemental Experimental Procedures](#) for details of bioinformatic analysis.

### ACCESSION NUMBERS

The accession number for the microarray data reported in this paper is GEO: GSE82308.

### SUPPLEMENTAL INFORMATION

Supplemental Information includes Supplemental Experimental Procedures, four figures, and one table and can be found with this article online at <http://dx.doi.org/10.1016/j.stem.2016.06.013>.

### AUTHOR CONTRIBUTIONS

V.S.-V. and F.D. designed experiments. A.R.M.-S., P.C., and V.S.-V. performed and analyzed experiments. D.M. and V.S.-V. performed bioinformatic analysis. V.S.-V. and F.D. wrote the paper.

### ACKNOWLEDGMENTS

We thank the F.D. and Wichterle labs for discussion; Z. Chaker, A. Delgado, A. DeLeo, and F. Favaloro for comments; and K. Gordon and S. Tetteh of Columbia University Herbert Irving Comprehensive Cancer Center (HICCC) for FACS. This work was supported by the Human Frontier Science Program Long-Term Fellowship (to V.S.-V.), NIH National Institute of Neurological Disorders and Stroke (NINDS) F31NS079057 (to A.R.M.-S.), NIH NINDS R01NS053884 (to F.D.), NIH NINDS F32NS090736 (to D.M.), NIH NINDS R01NS074039 (to F.D.), NIH NIA R21AG042671 (to F.D.), NYSTEM C024287 (to F.D.), NYSTEM C026401 (to F.D.), and The Leona M. and Harry B. Helmsley Charitable Trust (to F.D.). Work also was supported by the Jerry and Emily Spiegel Laboratory for Cell Replacement Therapies and the University of Basel.

Received: July 8, 2015

Revised: May 4, 2016

Accepted: June 20, 2016

Published: July 21, 2016

### REFERENCES

Azim, K., Fischer, B., Hurtado-Chong, A., Draganova, K., Cantù, C., Zemke, M., Sommer, L., Butt, A., and Raineteau, O. (2014). Persistent Wnt/ $\beta$ -catenin signaling determines dorsalization of the postnatal subventricular zone and neural stem cell specification into oligodendrocytes and glutamatergic neurons. *Stem Cells* 32, 1301–1312.

Baird, G.S., Nelson, S.K., Keeney, T.R., Stewart, A., Williams, S., Kraemer, S., Peskind, E.R., and Montine, T.J. (2012). Age-dependent changes in the cere-

brospinal fluid proteome by slow off-rate modified aptamer array. *Am. J. Pathol.* 180, 446–456.

Bartke, A., Sun, L.Y., and Longo, V. (2013). Somatotropic signaling: trade-offs between growth, reproductive development, and longevity. *Physiol. Rev.* 93, 571–598.

Baruch, K., Deczkowska, A., David, E., Castellano, J.M., Miller, O., Kertser, A., Berkutzki, T., Barnett-Itzhaki, Z., Bezalel, D., Wyss-Coray, T., et al. (2014). Aging. Aging-induced type I interferon response at the choroid plexus negatively affects brain function. *Science* 346, 89–93.

Bouab, M., Paliouras, G.N., Aumont, A., Forest-Bérard, K., and Fernandes, K.J. (2011). Aging of the subventricular zone neural stem cell niche: evidence for quiescence-associated changes between early and mid-adulthood. *Neuroscience* 173, 135–149.

Chen, C.P., Chen, R.L., and Preston, J.E. (2012). The influence of ageing in the cerebrospinal fluid concentrations of proteins that are derived from the choroid plexus, brain, and plasma. *Exp. Gerontol.* 47, 323–328.

Codega, P., Silva-Vargas, V., Paul, A., Maldonado-Soto, A.R., Deleo, A.M., Pastrana, E., and Doetsch, F. (2014). Prospective identification and purification of quiescent adult neural stem cells from their in vivo niche. *Neuron* 82, 545–559.

Conover, J.C., and Shook, B.A. (2011). Aging of the subventricular zone neural stem cell niche. *Aging Dis.* 2, 49–63.

Delgado, A.C., Ferrón, S.R., Vicente, D., Porlan, E., Perez-Villalba, A., Trujillo, C.M., D'Ocón, P., and Fariñas, I. (2014). Endothelial NT-3 delivered by vasculature and CSF promotes quiescence of subependymal neural stem cells through nitric oxide induction. *Neuron* 83, 572–585.

Fuentealba, L.C., Obernier, K., and Alvarez-Buylla, A. (2012). Adult neural stem cells bridge their niche. *Cell Stem Cell* 10, 698–708.

Johansson, P.A. (2014). The choroid plexuses and their impact on developmental neurogenesis. *Front. Neurosci.* 8, 340.

Kangsamaksin, T., and Morris, R.J. (2011). Bone morphogenetic protein 5 regulates the number of keratinocyte stem cells from the skin of mice. *J. Invest. Dermatol.* 131, 580–585.

Katsimpardi, L., Litterman, N.K., Schein, P.A., Miller, C.M., Loffredo, F.S., Wojtkiewicz, G.R., Chen, J.W., Lee, R.T., Wagers, A.J., and Rubin, L.L. (2014). Vascular and neurogenic rejuvenation of the aging mouse brain by young systemic factors. *Science* 344, 630–634.

Kokovay, E., Wang, Y., Kusek, G., Wurster, R., Lederman, P., Lowry, N., Shen, Q., and Temple, S. (2012). VCAM1 is essential to maintain the structure of the SVZ niche and acts as an environmental sensor to regulate SVZ lineage progression. *Cell Stem Cell* 11, 220–230.

Lehtinen, M.K., Zappaterra, M.W., Chen, X., Yang, Y.J., Hill, A.D., Lun, M., Maynard, T., Gonzalez, D., Kim, S., Ye, P., et al. (2011). The cerebrospinal fluid provides a proliferative niche for neural progenitor cells. *Neuron* 69, 893–905.

Lun, M.P., Monuki, E.S., and Lehtinen, M.K. (2015). Development and functions of the choroid plexus-cerebrospinal fluid system. *Nat. Rev. Neurosci.* 16, 445–457.

Marques, F., and Sousa, J.C. (2015). The choroid plexus is modulated by various peripheral stimuli: implications to diseases of the central nervous system. *Front. Cell. Neurosci.* 9, 136.

Marques, F., Sousa, J.C., Coppola, G., Gao, F., Puga, R., Brentani, H., Geschwind, D.H., Sousa, N., Correia-Neves, M., and Palha, J.A. (2011). Transcriptome signature of the adult mouse choroid plexus. *Fluids Barriers CNS* 8, 10.

Ortega, F., Gascón, S., Masserdotti, G., Deshpande, A., Simon, C., Fischer, J., Dimou, L., Chichung Lie, D., Schroeder, T., and Berninger, B. (2013). Oligodendroglial and neurogenic adult subependymal zone neural stem cells constitute distinct lineages and exhibit differential responsiveness to Wnt signalling. *Nat. Cell Biol.* 15, 602–613.

Ouzzine, M., Gulberti, S., Ramalanjaona, N., Magdalou, J., and Fournel-Gigleux, S. (2014). The UDP-glucuronosyltransferases of the blood-brain barrier: their role in drug metabolism and detoxication. *Front. Cell. Neurosci.* 8, 349.

- Pastrana, E., Cheng, L.C., and Doetsch, F. (2009). Simultaneous prospective purification of adult subventricular zone neural stem cells and their progeny. *Proc. Natl. Acad. Sci. USA* *106*, 6387–6392.
- Piccin, D., Tufford, A., and Morshead, C.M. (2014). Neural stem and progenitor cells in the aged subependyma are activated by the young niche. *Neurobiol. Aging* *35*, 1669–1679.
- Redzic, Z.B., Preston, J.E., Duncan, J.A., Chodobski, A., and Szmydynger-Chodobska, J. (2005). The choroid plexus-cerebrospinal fluid system: from development to aging. *Curr. Top. Dev. Biol.* *71*, 1–52.
- Sawamoto, K., Wichterle, H., Gonzalez-Perez, O., Cholfin, J.A., Yamada, M., Spassky, N., Murcia, N.S., Garcia-Verdugo, J.M., Marin, O., Rubenstein, J.L., et al. (2006). New neurons follow the flow of cerebrospinal fluid in the adult brain. *Science* *311*, 629–632.
- Signer, R.A., and Morrison, S.J. (2013). Mechanisms that regulate stem cell aging and life span. *Cell Stem Cell* *12*, 152–165.
- Silva-Vargas, V., Crouch, E.E., and Doetsch, F. (2013). Adult neural stem cells and their niche: a dynamic duo during homeostasis, regeneration, and aging. *Curr. Opin. Neurobiol.* *23*, 935–942.
- Strazielle, N., Creidy, R., Malcus, C., Boucraut, J., and Ghersi-Egea, J.F. (2016). T-Lymphocytes traffic into the brain across the blood-CSF barrier: evidence using a reconstituted choroid plexus epithelium. *PLoS ONE* *11*, e0150945.